Special Issue
"Protein-Ligand Interactions"

Vol. 13, pp. 173–180 (2016)
doi: 10.2142/biophysico.13.0_173

Biophysics and Physicobiology

https://www.jstage.jst.go.jp/browse/biophysico/

Regular Article

In silico studies for the interaction of tumor necrosis factor-alpha (TNF-α) with different saponins from Vietnamese ginseng (*Panax vietnamesis*)

Oanh T. P. Kim[1], Manh D. Le[2], Hoang X. Trinh[2] and Hai V. Nong[1]

[1]*Institute of Genome Research, Vietnam Academy of Science and Technology, Hanoi, 10000 Vietnam*
[2]*Center for Computational Physics, Institute of Physics, Vietnam Academy of Science and Technology, Hanoi, 10000 Vietnam*

Received January 8, 2016; accepted May 12, 2016

Tumor necrosis factor-alpha (TNF-α) is a cytokine that plays an important role in inflammatory process and tumor development. Recent studies demonstrate that triterpene saponins from Vietnamese ginseng are efficient inhibitors of TNF-α. But the interactions between TNF-α and the saponins are still unclear. In this study, molecular docking and molecular dynamics simulations of TNF-α with three different triterpene saponins (majonoside R2, vina-ginsenoside R1 and vina-ginsenoside R2) were performed to evaluate their binding ability. Our results showed that the triterpene saponins have a good binding affinity with protein TNF-α. The saponins were docked to the pore at the top of the "bell" or "cone" shaped TNF-α trimer and the complexes were structurally stable during 100 ns molecular dynamics simulation. The predicted binding sites would help to subsequently investigate the inhibitory mechanism of triterpene saponins.

Key words: ginsenosides, molecular docking, molecular dynamics simulation, TNF-α inhibitor

Corresponding author: Oanh T. P. Kim, Institute of Genome Research, Vietnam Academy of Science and Technology, 18 Hoang Quoc Viet, Cau Giay, Hanoi 10000, Vietnam.
e-mail: ktpoanh@igr.ac.vn

Vietnamese ginseng (*Panax vietnamesis*) is a valuable medical plant and indigenous to Vietnam. As other *Panax* plants (such as *P. ginseng*, *P. notoginseng*, *P. quinquefolium* and *P. japonicus*), the root or rhizome of *P. vietnamesis* has been used for treament of many serious diseases and for enhancing physical strength on human bodies. The main pharmacologically active substances of ginseng are saponins (known as ginsenosides) that contain a hydrophobic steroidal skeleton attached to hydrophilic sugar moieties or hydroxyl groups [1]. Compared with the most widely used ginseng *P. ginseng* which is indigenous to China and Korea, *P. vietnamesis* has more varieties of ginsenosides. Specially, majonoside-R2, the major saponin constituent from *P. vietnamesis*, has not been found in *P. ginseng*. Besides, many new dammarane saponins have been isolated from *P. vietnamesis* [2,3].

Ginseng saponins have been widely reported to have anti-inflammatory and anticancer activities. Studies showed that ginsenosides have ability to influence multiple signaling molecules. For examples, ginsenoside Rg1 was found to inhibit oncogenes c-myc, c-fos and downregulate nucleophosmin [4]; ginsenoside Rh1 suppresses inducible nitric oxide synthase (iNOS) gene expression which is involved in immune response [5] and increases expression of anti-

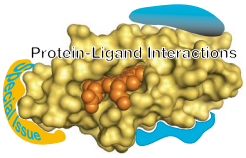

◀ Significance ▶

Among ginseng saponins, the ocotillol-type ginsenoside, especially majonoside-R2, from Vietnamese ginseng (*Panax vietnamesis*), had been found to have highest inhibitory effect on tumor necrosis factor-alpha (TNF-α). Our study predicted the binding modes of three different triterpene saponins (majonoside-R2, vina-ginsenoside R1 and vina-ginsenoside R2) to TNF-α, which will be helpful for further investigation of the inhibitory mechanism. The information at molecular level is very important for understanding the clinical advantages of the triterpene saponins.

inflammatory IL-10 and hemeoxygenase-1 (HO-1) [6]; Ginsenoside Rg1 and its metabolites ginsenoside Rh1 and 20(S)-protopanaxatriol were also found to inhibit the binding of lipopolysaccharide (LPS) to toll-like receptor 4 (TLR4) on the macrophages [7]; Ginsenoside Rg3 can significantly inhibit several kinds of tumor growth and metastasis [8–12]; Ginsenoside Rh2 was shown to have potent cell death activity [8,13]; Ginsenosides 25-OH-PPD and 25-OCH_3-PPD are also effective inhibitors of cell growth, proliferation and inducers of apoptosis [14–17]. Majonoside-R2, the ocotillol-type saponin isolated from the root and =rhizome of Vietnamese ginseng *P. vietnamesis*, exhibited cancer chemopreventive activity on two-stage carcinogenesis test of mouse hepatic tumor [18]. Majonoside-R2 and some other triterpene saponins from Vietnamese ginseng showed strong hepatocyte activities against D-galactosamine (D-GalN)/tumor necrosis factor-alpha (TNF-α)-induced cell death in primary cultured mouse hepatocytes [3]. In extensive experiments, TNF-α was significantly inhibited by majonoside-R2 [19]. Vina-ginsenoside-R2 and majonoside-R2 were also suggested to inhibit the binding of LPS to TLR4 on the macrophages that resulted in anti-inflammatory effects [20].

TNF-α is a cytokine secreted by macrophages in response to septic shock, inflammatory agents and cachexia. TNF-α is believed to play a key role in immune system and apoptosis [21–23]. TNF-α is involved in a number of autoimmune diseases, including psoriasis, inflammatory bowel disease, rheumatoid arthritis, systemic sclerosis, systemic lupus erythematosus, multiple sclerosis, diabetes and ankylosing spondylitis [22,23]. Since TNF-α is an important mediator in resistance against infections and tumors, a series of biological agents targeted to TNF-α have been introduced for treatment of cancer and autoimmunity [23,24]. The ginseng saponins are potential therapeutic agents, which can suppress TNF-α expression. Among these saponins, the ocotillol-type majonoside-R2 showed the highest inhibitory effect [20,25]

In order to identify protein targets of medicinal herbal ingredients, *in silico* method is a low-cost and rapid approach [26]. Molecular docking is the most commonly used computational tool for characterization of protein-ligand binding sites. A number of molecular modeling and docking studies have been done for predicting molecular targets and molecular mechanism of ginsenosides [27–31]. Based on the reported experimental evidence [3,19], we performed computational simulation of interactions between TNF-α and three triterpene saponins from Vietnamese ginseng (majonoside R2, vina-ginsenoside R1 and vina-ginsenoside R2). This study aims to examine the binding ability and obtain insight into the interactions.

Methods

Protein and ligand preparation

Three-dimensional structure of human TNF-α was retrieved from RCSB protein data bank [32]. The identification with 1TNF was hereafter used [21]. Homotrimer structure of TNF-α had determined using X-ray diffraction method at 2.6 Å resolution. The structure consists of three protein chains (A, B and C) without heteroatoms. For docking simulations, hydrogens were added onto the protein structure using AutoDockTools- 1.5.6 [33].

The 2D structures of the ligands, majonoside-R2, vina-ginsenoside-R1 and vina-ginsenoside-R2, were retrieved from the Pubchem Compound database from NCBI [34] with their respective PubChem CIDs: 44144327, 44144330 and 44593678. The 2D structures were converted into PDB format using an open source tool, Open Babel [35]. Hydrogen atoms were added into ligand structure and chemical bonds with capability of rotation were specified by AutoDockTools-1.5.6

Molecular docking

Dockings of TNF-α and ginseng saponins were performed using the AutoDock Vina software [36]. For each docking performace, a grid box was generated by fixing the number of points in x, y and z directions to 66 each. The spacing was adjusted to 1.00 Å. The center of the grid box was fixed to the point of (20, 50, 40).

Molecular dynamic simulation

Molecular dynamic (MD) simulation studies were carried out using the software package GROMACS [37] with the latest gromos force-field named 54a7. The topology for the ligands were created by the Automated Topology Builder (ATB) server [38]. The protein-ligand complex structure was put in a triclinic box in the way that every atom is more than 10 Å away from any box surfaces. Before starting the simulations, all the complex structures were solvated with the explicit simple point charge (SPC) water, and then were neutralized with sodium ions (number of added ions depends on each ligand). After that, the system was relaxed through energy minimization process by using steepest descent until reaching a tolerance of 1000 kJ/mol. The electrostatic interactions were estimated by using PME algorithm. The temperature and pressure conditions were stabilized with NVT and NPT ensembles by using modified Berendsen thermostat coupling and Parrinello-Rahman pressure coupling, respectively. Finally, the systems were simulated in water under the biological conditions, namely 300 K, approximately 1000 kg/m^3 water density and average pressure of 1 bar. The run time for each mode of complex was 100 ns.

Validation of the docking

In molecular docking, re-docking of co-crystallized ligand in protein is usually used for docking validation. In previous

study, x-ray crystal structure was solved for TNF-α- small molecule inhibitor complex [39]. The small molecule in this structure had displaced one of the subunits from the TNF-α trimer to form a complex with a dimer of TNF-α subunits (PDB ID: 2az5). The docking protocol will be changed if we re-dock the TNF-α dimer-inhibitor complex. In this work, we extracted the small molecule inhibitor from the complex (307 in PDB ID: 2az5) and performed docking with TNF-α trimer. However, it would be very difficult to simulate the conversion of TNF-α trimer to dimer because the reaction occurs in several hours. We can evaluate the binding affinity and the docking poses during 100 ns molecular dynamics simulation of TNF-α with the experimentally known small molecule inhibitor.

Results and Discussion

Molecular docking of TNF-α with saponins

Autodock Vina reports nine highest-affinity docking poses for each protein-ligand pair. The docking results were ranked according to the calculated binding energies as shown in Table 1. The estimated binding energies of majonoside-R2, vina-ginsenoside-R1 and vina-ginsenoside-R2 with TNF-α were within the range of –7.1 to –9.1 kcal/mol, which were similar to that of 307 with TNF-α (Table 1). Our results are also compatible with the docking results of a small molecular inhibitor with TNF-α in previous study (–8.57 kcal/mol) [40]. Based on these results, majonoside-R2, vina-ginsenoside-R1 and vina-ginsenoside-R2 were found to have a good binding affinity with protein TNF-α.

The docked results with majonoside-R2 showed that top three highest-affinity docking poses were located at the top of the "bell" or "cone" shape trimer (Supplementary Figure S1). The trimer is open at the top, forming a pore through the center of the TNF-α trimer [21]. The best mode showed that the sugar moiety of majonoside-R2 was inserted into pore and the steroidal skeleton protruded outside. The second best binding mode of majonoside-R2 had a reversed direction in which the steroidal skeleton was inserted into the pore. The third mode showed that majonoside-R2 tended to be on the surface rather than in the pore. In the 4th and 6th modes, majonoside-R2 was docked at different places on the surface of chain B. In the 5th mode, majonoside-R2 was docked at the surface of chain A. In the 7th and 8th modes, majonoside-R2 was docked at the bottom of the trimer. In the 9th mode, majonoside-R2 was docked at the edge formed between chains B and C.

Among nine docking modes for vina-ginsenoside-R1, five docking modes (1st, 2nd, 3rd, 5th and 8th) were located at the top of the TNF-α trimer (Supplementary Figure S2). The top three highest-affinity docking modes and the 5th mode showed the same docking direction in which the steroidal skeleton was inserted into the pore and the sugar moiety protruded outside. In the 8th mode, both steroidal skeleton and the sugar moiety of the ligand tended to be on the surface of the top of the trimer. In the 4th and 6th modes, vina-ginsenoside-R1 was docked at surface of chain B. In the 7th mode, vina-ginsenoside-R1 was docked at the edge between chain B and C. In the 9th mode, vina-ginsenoside-R1 was docked at surface of chain A.

The docked results with vina-ginsenoside-R2 showed that top two highest-affinity docking poses were located at the top of the TNF-α trimer (Supplementary Figure S3). Both of the two docking poses had the same docking direction in which the steroidal skeleton directed towards inside the pore of the trimer. In three docking modes (3rd, 4th and 7th), vina-ginsenoside-R2 was docked at different positions on the surface of the vertical edge between chain B and C. In

Table 1 Docking results of TNF-α and ligands

Ligands	Docking mode	Affinity (kcal/mol)	Distance from the best mode	
			RMSD lower bound	*RMSD upper bound*
majonoside-R2	1	–8.1	0.000	0.000
	2	–7.9	2.323	8.133
	3	–7.8	2.025	7.912
	4	–7.6	30.079	34.661
	5	–7.4	22.597	26.714
	6	–7.4	24.070	29.349
	7	–7.3	52.605	56.940
	8	–7.2	47.917	52.797
	9	–7.2	24.015	27.681
vina-ginsenoside R1	1	–9.1	0.000	0.000
	2	–8.9	1.628	3.752
	3	–8.1	3.316	7.289
	4	–7.7	17.325	22.849
	5	–7.6	3.461	7.220
	6	–7.5	17.589	22.081
	7	–7.5	22.290	28.660
	8	–7.3	6.370	9.837
	9	–7.3	20.147	23.784
vina-ginsenoside R2	1	–8.1	0.000	0.000
	2	–7.9	3.610	6.774
	3	–7.7	27.581	33.776
	4	–7.5	45.359	48.707
	5	–7.3	22.874	29.469
	6	–7.3	20.954	27.084
	7	–7.2	27.729	34.115
	8	–7.2	25.573	31.254
	9	–7.1	22.827	28.149
307	1	–9.0	0.000	0.000
	2	–9.0	5.323	11.245
	3	–8.6	4.528	10.735
	4	–8.5	2.802	5.349
	5	–8.4	3.759	5.869
	6	–8.3	2.919	4.893
	7	–8.1	3.481	6.662
	8	–7.9	29.690	33.873
	9	–7.8	23.072	26.614

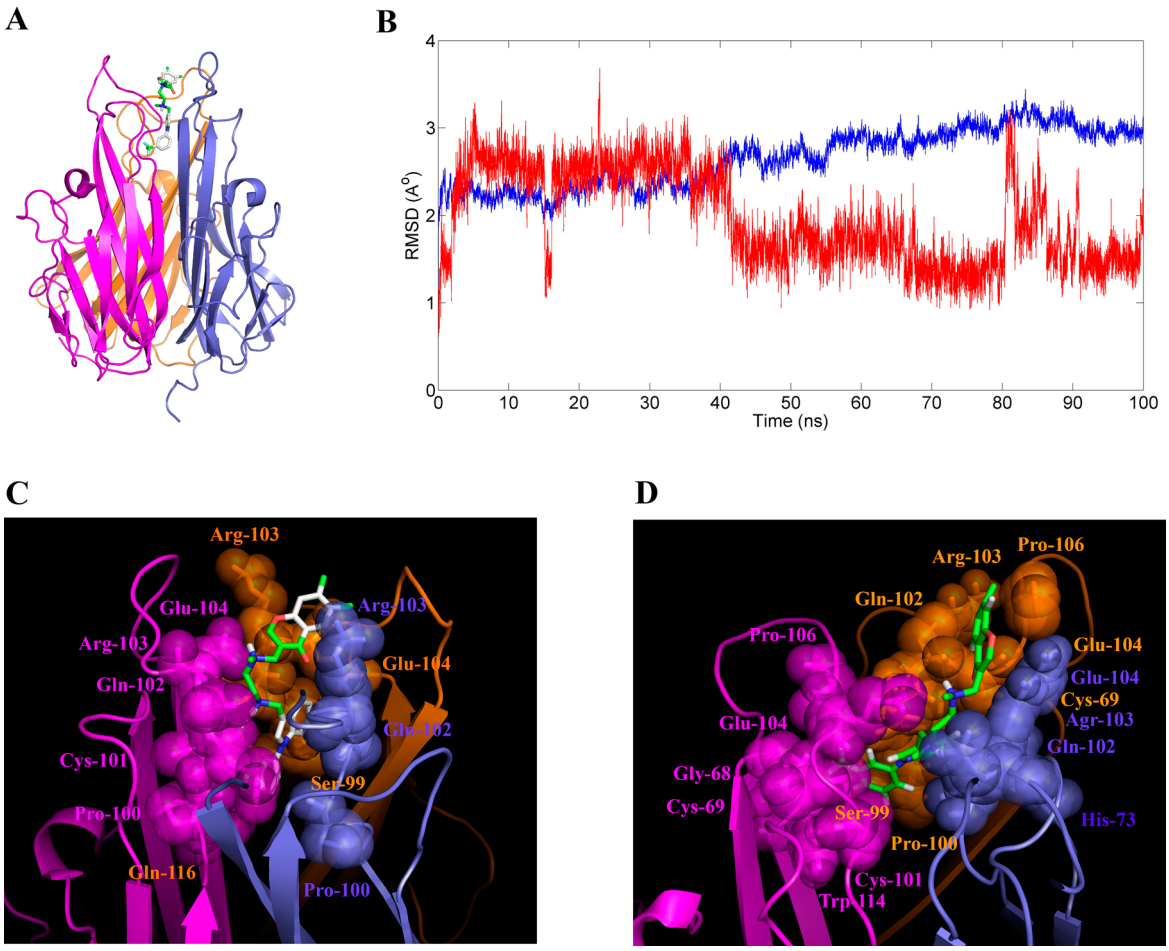

Figure 1 Docking and MD simulation of TNF-α with the experimentally known small molecule inhibitor (307). A. The best mode of docking results with 307; B. RMSD vs. time plot; C. Binding site of 307 at 0 ns of MD simulation (docked pose); and D. Binding site of 307 at 90 ns of MD simulation. Chains A, B and C of TNF-α are coloured in magentas, slate-blue and orange, respectively. The residues which interact with ligand are displayed in spheres. The ligands are displayed in stick model. In B figure, the blue curves are RMSD of the protein (TNF-α) and the red curves are the RMSDs of ligand (307)

the 6th mode, vina-ginsenoside-R2 is docked at surface of chain A. In three docking modes (5th, 8th and 9th), vina-ginsenoside-R2 is docked at different positions on the surface of chain B.

Among nine docking modes for 307, seven docking modes (from 1st to 7th) were located into the pore at the top of the TNF-α trimer. Figure 1A shows the best binding modes of 307. Overall, the best modes of all ligands were docked into the same binding pocket of the protein. These results strongly suggest that the pore of the TNF-α trimer should be the accceptor for saponin molecules.

Molecular dynamic simulation

In order to search for the best modes of TNF-α trimer and saponin interactions, we have performed molecular dynamics (MD) simulations. The root mean square deviation (RMSD) values of both protein and ligand along 100 ns MD trajectories were monitored to assess the dynamic stability of the protein-ligand complex.

For the experimentally known ligand (307), the RMSD curves for protein fluctuated below 3.0 Å, while the RMSD curves for ligand were lower (Fig. 1B). That means the ligand 307 is quite stable in this pose. After 90 ns of MD simulation, the ligand 307 was still in the pocket and able to have interaction with hydrophobic amino acids that located inside the pore such as Gly68, Cys69, Cys101, and Trp114 (Fig. 1C and D).

For the studied triterpene saponins, we performed MD simulations for the top three highest-affinity docking modes of each ligand. Figure 2 shows RMSD curves for the cases. In all the simulations for the TNF-α–majonoside-R2 complex, the RMSDs for protein stayed below 2.5 Å throughout the simulation and they reached a plateau after the first few ns, which means that the MD trajectories appeared to be well equilibrated. The fluctuation of RMSDs of the ligand was quite similar to that of proteins in the complex of 1st and 2nd binding mode (Fig. 2: A-1, A-2). However, in the simulation started with modes 3 (Fig. 2: A-3), the RMSD fluctuations of

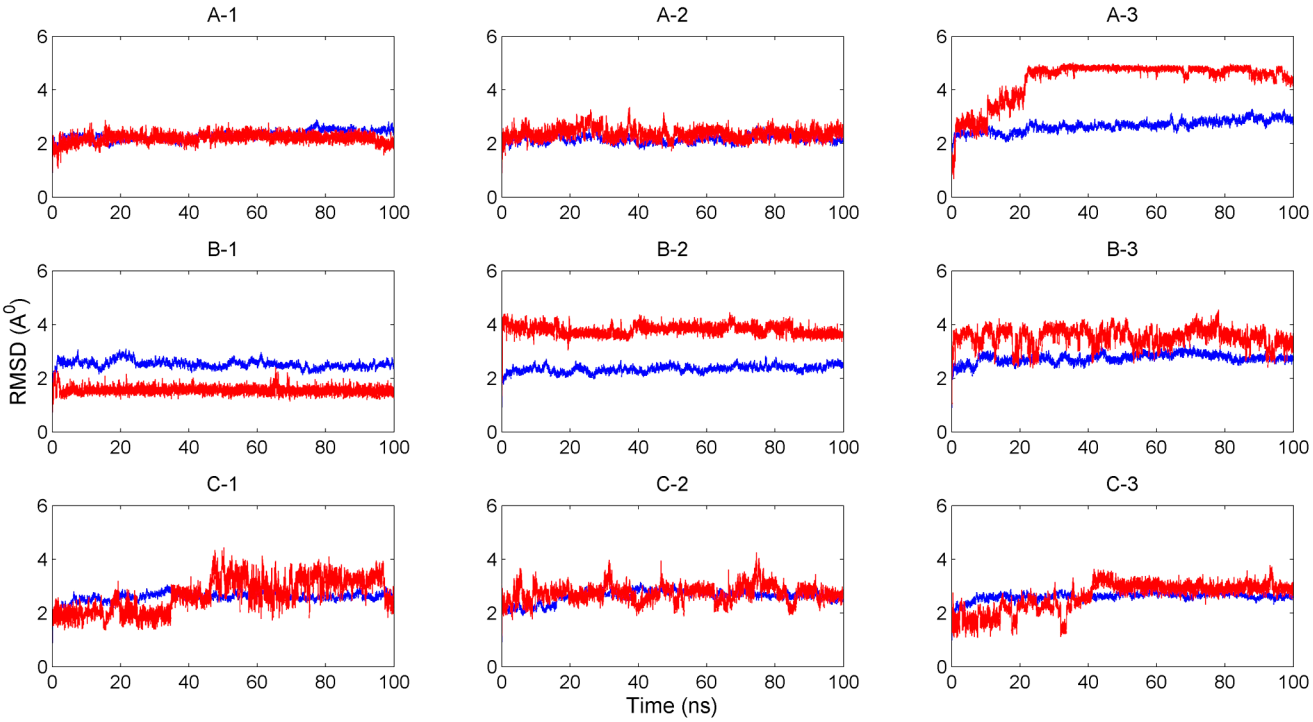

Figure 2 RMSD vs. time plots. The blue curves are RMSD of the protein (TNF-α) and the red curves are the RMSDs of ligands. A-1, A-2, A-3 show the plots of the top three highest-affinity docking modes of majonoside-R2. B-1, B-2, B-3 show the plots of the top three highest-affinity docking modes of vina-ginsenoside-R1. C-1, C-2, C-3 show the plots of the top three highest-affinity docking modes of vina-ginsenoside-R2.

ligand were much higher (>4 Å), which suggests that the ligand interaction should be less stable than those of 1st and 2nd modes.

The MD simulation results with the TNF-α–vina-ginsenoside-R1 complex showed that the RMSD curves for protein fluctuated below 2.5 Å in all modes, while the RMSD curves for ligand were different from one another (Fig. 2: B-1, B-2 and B-3). In the 1st mode, the average RMSD value of ligand was the lowest (<2 Å), which means that the fluctuation of the ligand is very confined in this pose. Vina-ginsenoside-R1 is more flexible in the second and the third modes.

The MD simulation results with the TNF-α–vina-ginsenoside-R2 complex also showed that the RMSD values of protein were around 2.5 Å, while the RMSD values of the ligand had more fluctuation (Fig. 2: C1, C2 and C3). Vina-ginsenoside-R2 in the 2nd mode is more stable than those in other modes.

The MD trajectories of the best modes for each complex kept within 3.0 Å against the starting structure, which suggests that the complexes should be structurally stable. The MD simulation results show that binding mode of the protein-ligand interaction was nearly the same as in molecular docking.

Binding sites of the three triterpene saponins and TNF-α

To get an insight into the interactions between the three triterpene saponins and TNF-α, we observed and analyzed the predicted binding sites. Figure 3 shows snapshots of binding sites at 90 ns of MD simulations for the best binding modes. All three ligands have the same docking direction in which the steroidal skeleton was inserted into the pore and the sugar moiety directed towards outside (Fig. 3). The binding sites consist of residues in the flexible loops at the top of the TNF-α trimer (residues 102–112 in each chain). The sugar moieties of the ligands can form hydrogen bonds with surface residues Gln102, Arg103, Glu104, Thr105 and Glu107. The steroidal skeleton can have hydrophobic interaction with the residues located inside the pore Cys69, Pro100, Cys101, Ala109, Pro113 and Trp114.

For treating TNF-α associated disease, a number of anti-TNF-α agents have been developed such as Etanercept (a soluble TNF receptor), Infliximab (a mouse-human chimera anti-TNF antibodies), and Adalimumab (a human anti-TNF antibodies) [23]. The crystal structure of the Infliximab Fab fragment in complex with TNF-α revealed that the loop from residues 102–112, namely E-F loop, played a crucial role in the interactions between antibody Infliximab and TNF-α [41]. The E-F loop has distinct features that specifies the binding of infliximab to TNF-α but not TNF-β. Residues Thr105, Glu107, Ala109 and Glu110 in E-F loop take part in interactions between TNF-α and Infliximab as well as Adalimumab [42]. However, there is no evidence to show how this loop is important to the biological function of

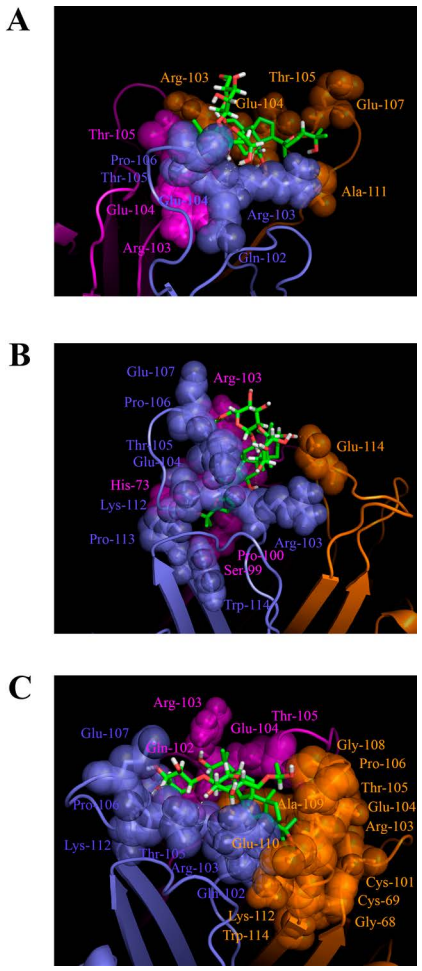

Figure 3 Binding sites of the studied triterpene saponins and TNF-α. A. Binding sites of majonoside-R2; B. Binding sites of vina-ginsenoside-R1; and C. Binding sites of vina-ginsenoside-R2. Chains A, B and C of TNF-α are coloured in magentas, slate-blue and orange, respectively. The residues which interact with ligand are displayed in spheres. The ligands are displayed in stick model.

TNF-α [41]. In a previous study, a compound composed of triflurometh ylphenyl indole and dimethyl chromone moieties linked by dimethylamine spacer ($C_{32}H_{32}F_3N_3O_2$) was found to inhibit TNF-α activity (307 in PDB ID: 2az5). The X-ray crystal structure of the TNF-α-compound complex reveals that the small molecule TNF-α inhibitor contacts residues that are buried in the TNF-α trimer and promotes subunit dissociation process [39]. In this sudy, the docking with TNF-α trimer of 307, the small molecular inhibitor, was performed. Athough the molecular structure of the triterpene saponin is a bit bigger than 307, the docking showed similar results in which the ligand was docked into the pore at the top of the TNF-α trimer. This leads to a speculation that the triterpene saponins are also able to access the interior of TNF-α trimer. The present study suggests that the binding of triterpene saponins should have indirect impact to the function of TNF-α, and should affect the formation of TNF-α trimer. The mechanism by which the triterpene saponins function remains to be elucidated.

Conclusion

The extremely high yield of ocotillol-type ginsenoside, especially majonoside-R2 has made Vietnamese ginseng (*Panax vietnamensis*) an valuable traditional medicine among *Panax* species. Our study predicted the binding modes of majonoside-R2, vina-ginsenoside R1 and vina-ginsenoside R2 to TNF-α for the first time. The predicted binding sites will be helpful for further investigation of the inhibitory mechanism.

Acknowledgement

This work has been supported by project "*Development of problem-solving environments for computational science based on resource sharing high-performance computers at Vietnam Academy of Science and Technology*" from Vietnam Academy of Science and Technology.

Conflicts of Interest

All authors declare that they have no conflict of interest.

Author Contributions

O. T. P. K., H. X. T., and H. V. N. planned this project. O. T. P. K and M. D. L. performed the calculation and wrote the manuscript.

References

[1] Nag, S. A., Qin, J. J., Wang, W., Wang, M. H., Wang, H. & Zhang, R. Ginsenosides as Anticancer Agents: In vitro and in vivo Activities, Structure-Activity Relationships, and Molecular Mechanisms of Action. *Front. Pharmacol.* **3**, 25 (2012).
[2] Duc, N. M., Kasai, R., Ohtani, K., Ito, A., Nham, N. T., Yamasaki, K., *et al.* Saponins from Vietnamese ginseng, Panax vietnamensis Ha et Grushv. collected in central Vietnam. III. *Chem. Pharm. Bull. (Tokyo)* **42**, 634–640 (1994).
[3] Tran, Q. L., Adnyana, I. K., Tezuka, Y., Nagaoka, T., Tran, Q. K. & Kadota, S. Triterpene saponins from Vietnamese ginseng (Panax vietnamensis) and their hepatocytoprotective activity. *J. Nat. Prod.* **64**, 456–461 (2001).
[4] Li, Q. F., Shi, S. L., Liu, Q. R., Tang, J., Song, J. & Liang, Y. Anticancer effects of ginsenoside Rg1, cinnamic acid, and tanshinone IIA in osteosarcoma MG-63 cells: nuclear matrix downregulation and cytoplasmic trafficking of nucleophosmin. *Int. J. Biochem. Cell Biol.* **40**, 1918–1929 (2008).
[5] Jung, J. S., Kim, D. H. & Kim, H. S. Ginsenoside Rh1 suppresses inducible nitric oxide synthase gene expression in IFN-gamma-stimulated microglia via modulation of JAK/STAT and ERK signaling pathways. *Biochem. Biophys. Res. Commun.* **397**, 323–328 (2010).
[6] Jung, J. S., Shin, J. A., Park, E. M., Lee, J. E., Kang, Y. S., Min, S. W., *et al.* Anti-inflammatory mechanism of ginsenoside Rh1 in lipopolysaccharide-stimulated microglia: critical role of the

protein kinase A pathway and hemeoxygenase-1 expression. *J. Neurochem.* **115**, 1668–1680 (2010).
[7] Lee, S. Y., Jeong, J. J., Eun, S. H. & Kim, D. H. Anti-inflammatory effects of ginsenoside Rg1 and its metabolites ginsenoside Rh1 and 20(S)-protopanaxatriol in mice with TNBS-induced colitis. *Eur. J. Pharmacol.* **762**, 333–343 (2015).
[8] Kim, H. S., Lee, E. H., Ko, S. R., Choi, K. J., Park, J. H. & Im, D. S. Effects of ginsenosides Rg3 and Rh2 on the proliferation of prostate cancer cells. *Arch. Pharm. Res.* **27**, 429–435 (2004).
[9] Wang, X., Zheng, Y. L., Li, K., Lin, N. & Fan, Q. X. [The effects of ginsenosides Rg3 on the expressions of VEGF and KDR in human lung squamous cancer cells]. *Zhong Yao Cai* **32**, 1708–1710 (2009).
[10] Wang, X., Zheng, Y. L., Li, K., Lin, N. & Fan, Q. X. [Ginsenoside Rg3 induces apoptosis of human lung squamous cell carcinoma SK-MES-1 cell line]. *Nan Fang Yi Ke Da Xue Xue Bao* **29**, 1823–1826 (2009).
[11] Xu, T. M., Cui, M. H., Xin, Y., Gu, L. P., Jiang, X., Su, M. M., *et al.* Inhibitory effect of ginsenoside Rg3 on ovarian cancer metastasis. *Chin. Med. J. (Engl.)* **121**, 1394–1397 (2008).
[12] Xu, T. M., Xin, Y., Cui, M. H., Jiang, X. & Gu, L. P. Inhibitory effect of ginsenoside Rg3 combined with cyclophosphamide on growth and angiogenesis of ovarian cancer. *Chin. Med. J. (Engl.)* **120**, 584–588 (2007).
[13] Li, B., Zhao, J., Wang, C. Z., Searle, J., He, T. C., Yuan, C. S., *et al.* Ginsenoside Rh2 induces apoptosis and paraptosis-like cell death in colorectal cancer cells through activation of p53. *Cancer Lett.* **301**, 185–192 (2011).
[14] Wang, W., Zhao, Y., Rayburn, E. R., Hill, D. L., Wang, H. & Zhang, R. In vitro anti-cancer activity and structure-activity relationships of natural products isolated from fruits of Panax ginseng. *Cancer Chemother. Pharmacol.* **59**, 589–601 (2007).
[15] Wang, W., Rayburn, E. R., Zhao, Y., Wang, H. & Zhang, R. Novel ginsenosides 25-OH-PPD and 25-OCH3-PPD as experimental therapy for pancreatic cancer: anticancer activity and mechanisms of action. *Cancer Lett.* **278**, 241–248 (2009).
[16] Wang, W., Zhang, X., Qin, J. J., Voruganti, S., Nag, S. A., Wang, M. H., *et al.* Natural Product Ginsenoside 25-OCH(3)-PPD Inhibits Breast Cancer Growth and Metastasis through Down-Regulating MDM2. *PLoS ONE* **7**, e41586 (2012).
[17] Zhao, Y., Wang, W., Han, L., Rayburn, E. R., Hill, D. L., Wang, H., *et al.* Isolation, structural determination, and evaluation of the biological activity of 20(S)-25-methoxyl-dammarane-3β, 12β, 20-triol [20(S)-25-OCH3-PPD], a novel natural product from Panax notoginseng. *Med. Chem.* **3**, 51–60 (2007).
[18] Konoshima, T., Takasaki, M., Ichiishi, E., Murakami, T., Tokuda, H., Nishino, H., *et al.* Cancer chemopreventive activity of majonoside-R2 from Vietnamese ginseng, Panax vietnamensis. *Cancer Lett.* **147**, 11–16 (1999).
[19] Tran, Q. L., Adnyana, I. K., Tezuka, Y., Harimaya, Y., Saiki, I., Kurashige, Y., *et al.* Hepatoprotective effect of majonoside R2, the major saponin from Vietnamese ginseng (Panax vietnamensis). *Planta Med.* **68**, 402–406 (2002).
[20] Jeong, J. J., Van Le, T. H., Lee, S. Y., Eun, S. H., Nguyen, M. D., Park, J. H., *et al.* Anti-inflammatory effects of vina-ginsenoside R2 and majonoside R2 isolated from Panax vietnamensis and their metabolites in lipopolysaccharide-stimulated macrophages. *Int. Immunopharmacol.* **28**, 700–706 (2015).
[21] Eck, M. J. & Sprang, S. R. The structure of tumor necrosis factor-alpha at 2.6 A resolution. Implications for receptor binding. *J. Biol. Chem.* **264**, 17595–17605 (1989).
[22] Idriss, H. T. & Naismith, J. H. TNF alpha and the TNF receptor superfamily: structure-function relationship(s). *Microsc. Res. Tech.* **50**, 184–195 (2000).
[23] Sethi, G., Sung, B., Kunnumakkara, A. B. & Aggarwal, B. B. Targeting TNF for Treatment of Cancer and Autoimmunity. *Adv. Exp. Med. Biol.* **647**, 37–51 (2009).
[24] Caminero, A., Comabella, M. & Montalban, X. Tumor necrosis factor alpha (TNF-α), anti-TNF-α and demyelination revisited: an ongoing story. *J. Neuroimmunol.* **234**, 1–6 (2011).
[25] Lee, S. Y., Jeong, J. J., Le, T. H., Eun, S. H., Nguyen, M. D., Park, J. H., *et al.* Ocotillol, a Majonoside R2 Metabolite, Ameliorates 2,4,6-Trinitrobenzenesulfonic Acid-Induced Colitis in Mice by Restoring the Balance of Th17/Treg Cells. *J. Agric. Food Chem.* **63**, 7024–7031 (2015).
[26] Chen, X., Ung, C. Y. & Chen, Y. Can an in silico drug-target search method be used to probe potential mechanisms of medicinal plant ingredients? *Nat. Prod. Rep.* **20**, 432–444 (2003).
[27] Chen, R. J., Chung, T. Y., Li, F. Y., Lin, N. H. & Tzen, J. T. Effect of sugar positions in ginsenosides and their inhibitory potency on Na+/K+-ATPase activity. *Acta Pharmacol. Sin.* **30**, 61–69 (2009).
[28] Qu, C., Yu, S., Bai, A. & Wang, J. Study on the interactions between ginsenosides and lysozyme under acidic condition by ESI-MS and molecular docking. *Spectrochim. Acta A Mol. Biomol. Spectrosc.* **78**, 676–680 (2010).
[29] Sathishkumar, N., Sathiyamoorthy, S., Ramya, M., Yang, D. U., Lee, H. N. & Yang, D. C. Molecular docking studies of anti-apoptotic BCL-2, BCL-XL, and MCL-1 proteins with ginsenosides from Panax ginseng. *J. Enzyme. Inhib. Med. Chem.* **27**, 685–692 (2011).
[30] Karpagam, V., Sathishkumar, N., Sathiyamoorthy, S., Rasappan, P., Shila, S., Kim, Y. J., *et al.* Identification of BACE1 inhibitors from Panax ginseng saponins-An Insilco approach. *Comput. Biol. Med.* **43**, 1037–1044 (2013).
[31] Sathishkumar, N., Karpagam, V., Sathiyamoorthy, S., Woo, M. J., Kim, Y. J. & Yang, D. C. Computer-aided identification of EGFR tyrosine kinase inhibitors using ginsenosides from Panax ginseng. *Comput. Biol. Med.* **43**, 786–797 (2013).
[32] Berman, H. M., Westbrook, J., Feng, Z., Gilliland, G., Bhat, T. N., Weissig, H., *et al.* The Protein Data Bank. *Nucleic Acids Res.* **28**, 235–242 (2000).
[33] Morris, G. M., Huey, R., Lindstrom, W., Sanner, M. F., Belew, R. K., Goodsell, D. S., *et al.* AutoDock4 and AutoDockTools4: Automated docking with selective receptor flexibility. *J. Comput. Chem.* **30**, 2785–2791 (2009).
[34] Wang, Y., Xiao, J., Suzek, T. O., Zhang, J., Wang, J. & Bryant, S. H. PubChem: a public information system for analyzing bioactivities of small molecules. *Nucleic Acids Res.* **37**, W623–633 (2009).
[35] Geldenhuys, W. J., Gaasch, K. E., Watson, M., Allen, D. D. & Van der Schyf, C. J. Optimizing the use of open-source software applications in drug discovery. *Drug Discov. Today* **11**, 127–132 (2006).
[36] Trott, O. & Olson, A. J. AutoDock Vina: improving the speed and accuracy of docking with a new scoring function, efficient optimization, and multithreading. *J. Comput. Chem.* **31**, 455–461 (2010).
[37] Van Der Spoel, D., Lindahl, E., Hess, B., Groenhof, G., Mark, A. E. & Berendsen, H. J., GROMACS: fast, flexible, and free. *J. Comput. Chem.* **26**, 1701–1718 (2005).
[38] Koziara, K. B., Stroet, M., Malde, A. K. & Mark, A. E. Testing and validation of the Automated Topology Builder (ATB) version 2.0: prediction of hydration free enthalpies. *J. Comput. Aided Mol. Des.* **28**, 221–233 (2014).
[39] He, M. M., Smith, A. S., Oslob, J. D., Flanagan, W. M., Braisted, A. C., Whitty, A., *et al.* Small-molecule inhibition of TNF-alpha. *Science* **310**, 1022–1025 (2005).
[40] Kumar, K. S., Kumar, P. M., Kumar, K. A., Sreenivasulu, M.,

Jafar, A. A., Rambabu, D., *et al.* A new three-component reaction: green synthesis of novel isoindolo[2,1-a]quinazoline derivatives as potent inhibitors of TNF-α. *Chem. Commun. (Camb.)* **47**, 5010–5012 (2011).
[41] Liang, S., Dai, J., Hou, S., Su, L., Zhang, D., Guo, H., *et al.* Structural basis for treating tumor necrosis factor alpha (TNFalpha)-associated diseases with the therapeutic antibody infliximab. *J. Biol. Chem.* **288**, 13799–13807 (2013).
[42] Hu, S., Liang, S., Guo, H., Zhang, D., Li, H., Wang, X., *et al.* Comparison of the inhibition mechanisms of adalimumab and infliximab in treating tumor necrosis factor α-associated diseases from a molecular view. *J. Biol. Chem.* **288**, 27059–27067 (2013).